Research Article

Synaptic remodeling in mouse motor cortex after spinal cord injury

https://doi.org/10.4103/1673-5374.295346

Received: March 17, 2020

Peer review started: March 24, 2020

Accepted: April 23, 2020

Published online: October 9, 2020

Ke-Xue Zhang[1, #], Jia-Jia Zhao[2, #], Wei Chai[3, *], Ji-Ying Chen[3, *]

Graphical Abstract *Synapse remodeling in motor cortex after spinal cord hemi-section*

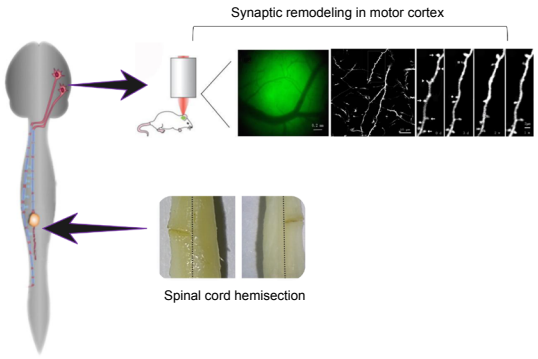

Abstract

Spinal cord injury dramatically blocks information exchange between the central nervous system and the peripheral nervous system. The resulting fate of synapses in the motor cortex has not been well studied. To explore synaptic reorganization in the motor cortex after spinal cord injury, we established mouse models of T12 spinal cord hemi-section and then monitored the postsynaptic dendritic spines and presynaptic axonal boutons of pyramidal neurons in the hindlimb area of the motor cortex *in vivo*. Our results showed that spinal cord hemi-section led to the remodeling of dendritic spines bilaterally in the motor cortex and the main remodeling regions changed over time. It made previously stable spines unstable and eliminated spines more unlikely to be re-emerged. There was a significant increase in new spines in the contralateral motor cortex. However, the low survival rate of the new spines demonstrated that new spines were still fragile. Observation of presynaptic axonal boutons found no significant change. These results suggest the existence of synapse remodeling in motor cortex after spinal cord hemi-section and that spinal cord hemi-section affected postsynaptic dendritic spines rather than presynaptic axonal boutons. This study was approved by the Ethics Committee of Chinese PLA General Hospital, China (approval No. 201504168S) on April 16, 2015.

Key Words: central nervous system; plasticity; recovery; regeneration; repair; spinal cord injury; synapses

Chinese Library Classification No. R446; R741; R363

Introduction

Spinal cord injury (SCI) is a serious condition, which blocks the normal message transfer of motor outputs and sensory inputs between the cortex and the body. Increasing evidence indicates that the recovery mechanism after SCI is not limited to the spinal cord but spans a large-scale network in supraspinal regions (Isa, 2017; Brown and Martinez, 2019; Grau et al., 2020). Nardone et al. (2018) reported that SCI led to cortical morphometric changes. However, the anatomical basis and mechanism that underlie these changes, which is crucial for developing comprehensive evidence-based therapies for SCI, have not been thoroughly examined (Kramer et al., 2012; Nardone et al., 2018).

Synapses, the basic building blocks of neural connections and the transfer hub of information between neurons, are composed of presynaptic axonal boutons and postsynaptic dendritic spines and both are important indicators of the reorganization in neural connections (Segal, 2005; Tada and Sheng, 2006; Harms and Dunaevsky, 2007; Lemtiri-Chlieh et al., 2011; Yu and Zuo, 2011; Chen et al., 2014; Cao et al., 2015; Hu et al., 2019). The morphology and population of spines are sensitive to various environmental or experienced stimuli (Kim et al., 2008; Johnston, 2009). Owing to their potential malleable nature, synapses may represent a key substrate of neuronal plasticity that underlies brain rewiring and recovery after injury (Li et al., 2007). There have been *in vitro* postmortem histological studies which showed that SCI induced changes in spine density (Kim et al., 2006; Ghosh et al., 2012). However, these studies could only provide

[1]Department of Pediatric Surgery, Chinese PLA General Hospital, Beijing, China; [2]Department of Anesthesiology, Shunyi District Hospital, Beijing, China; [3]Department of Orthopedics, Chinese PLA General Hospital, Beijing, China

***Correspondence to:** Ji-Ying Chen, MD, 570457036@qq.com; Wei Chai, MD, chaiwei301@163.com.

https://orcid.org/0000-0001-8166-4658 (Ji-Ying Chen); https://orcid.org/0000-0001-8781-9745 (Wei Chai); https://orcid.org/0000-0002-6419-2553 (Ke-Xue Zhang)

#Both authors contributed equally to this study.

Funding: *This work was supported by grants of Foundation and Strengthening Program in Technical Area of China, No. 2019-JCJQ-JJ-149 (to KXZ); and Military Medical Youth Program of Chinese PLA General Hospital, No. QNF19056 (to KXZ).*

How to cite this article: *Zhang KX, Zhao JJ, Chai W, Chen JY (2021) Synaptic remodeling in mouse motor cortex after spinal cord injury. Neural Regen Res 16(4):744-749.*

endpoint measures of reorganization and identify a fraction of changes in spine density rather than detail the turnover of synapses and the process of reorganization. Most previous related studies compared fixed cortical slices, excluding the possibility of monitoring changes in an individual synapse in real-time. In addition, the targets of previous studies of SCI were limited to postsynaptic dendritic spines; few of them focused on presynaptic axonal boutons. It is to be expected that the modifications of axonal boutons also participate in cortex plasticity (Yu and Zuo, 2011). There are several major problems to be solved: (1) Is there difference of reorganization between post-synaptic dendritic spines and pre-synaptic axonal boutons? (2) What is the difference of reorganization between the ipsi- and contra-lateral motor cortices after spinal cord hemi-section (SPH)? (3) What happened to the three kinds of dendritic spines (stable spines, new spines and eliminated spines) after SPH?

High-resolution and time-lapse transcranial two-photo imaging techniques, combined with fluorescent technology make it possible to image a synapse longitudinally and repeatedly in living animals (Grutzendler et al., 2002; Pan and Gan, 2008; Lai et al., 2018; Xu et al., 2019). In this study, we used a thinned skull protocol (Zhang et al., 2015) and transgenic fluorescent mice to monitor *in vivo* the turnover of presynaptic axonal boutons and postsynaptic dendritic spines in the hindlimb (HL) motor cortex. The fate of synapses in the HL motor cortex was continually monitored for 1 month after SPH.

Materials and Methods

Animals

The transgenic male mice (Thy1-YFP) which were provide by Institute of Laboratory Animal Sciences, Chinese Academy of Medical Sciences (license No. 2013-0002), were clean, healthy, 1 month old, and weighed 10–15 g. Twelve male mice were randomly divided into control and SPH groups with six mice in each group. Additional three mice were used to check the SPH model. The experiment methods were approved by the Ethics Committee of General Hospital of Chinese People's Liberation Army (approval No. 201504168S) on April 16, 2015. All surgeries were performed under the anesthesia of sodium pentobarbital (10.0 mL/kg; Shanghai Xinyu Biotechnology Company, Shanghai, China) and all efforts were made to minimize the suffering of mice. The mice were caged in each cage. The conditions were not specially used to encourage return of motor function. The mice were caged under standard room temperature and humidity, with a 12-hour dark-light cycle and had free access to food and fresh water throughout the experiment. The general appearance, demeanor, body weight, coat condition, posture, diet information and responses to handling of mice were checked every day. We scrutinized every mouse to make sure that there is no infection or unexpected injury in mice.

Establishment of spinal cord hemi-section model

The procedure of the SPH has been described in a previous study (Zhang et al., 2015). An anatomical microscope (Beijing Ce Wei Optoelectronic instrument company, Beijing, China) was used during all the surgery. After laminectomy of the vertebrae (thoracic (T) 11–12), the left hemisphere of T12 was hemisected from dorsal to ventral direction with a microblade (**Figure 1A**). It was cut twice and confirmed visually by the complete separation of the transected terminals to ensure the complete hemisection. Three mice were euthanized for histological analyses of the SPH (**Figure 1B**). In the sham group, only laminectomy of T11–12 was performed.

Behavioral assessment

Mean Basso Mouse Scale (BMS) scores for locomotion and BMS subscores for locomotion (Basso et al., 2006) were used to assess the HL function at 12 hours, 3 days, 2 weeks, and 1 month. HL motor activity was evaluated for 5 minutes in a 76.2 × 91.4 cm^2 enclosure. Two trained observers assessed the scores with an interrater reliability ≥ 95%. The BMS scores ranged from 0 (no ankle movement) to 9 (frequent or consistent plantar stepping, mostly coordinated, paws parallel at initial contact and lift off, normal trunk stability and tail always up). The BMS subscores ranged from 0 to 11.

Mouse head grinding and fixation

The method of grinding and fixation has been reported previously (Zhang et al., 2015). After the anesthesia of sodium pentobarbital (10.0 mL/kg), the desired area was exposed by incising the scalp along the middle of skull. To minimize respiration-induced movements, cyanoacrylate (Dongguan Yihe New Material Technology Company, Dongguan, China) was used to fix the steel sheet onto the desired area (**Figure 2A**). A gap in the middle of the steel sheet enabled convenient observation of the desired area. Then, the head of mouse was held by metal bases located on both sides of the head. The target region was ground with a high-speed drill under an anatomical microscope (**Figure 2B**). The desired area of the skull was thinned carefully. During grinding, artificial cerebrospinal fluid is used intermittently to prevent frictional heat-induced intracranial injury. After grinding, a micro-blade was used to scrape the surface of the desired area. The thickness of the skull in the desired area was reduced to approximately 10–20 μm to acquire the best imaging quality. During grinding and scraping, two-photon microscopy (Shanghai Terer Optoelectronics Company, Shanghai, China) was used to measure and ensure that the correct thickness of the desired area of the skull was achieved (**Figure 2C**). The total procedure lasted approximately half an hour.

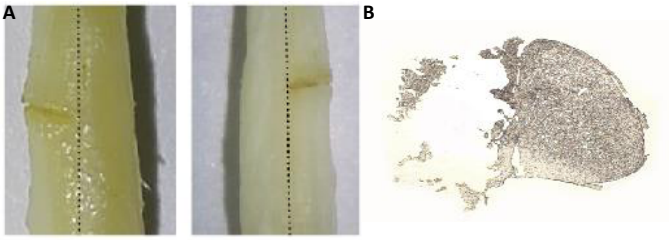

Figure 1 | **Hemisection of T12 in the spinal cord.**
(A) The hemisection of T12 in the spinal cord (view from the dorsal (left) and ventral (right) sides). The black dotted line indicates the center of the spinal cord. (B) The horizontal section shows the complete hemisection of T12. T12: Thoracic 12.

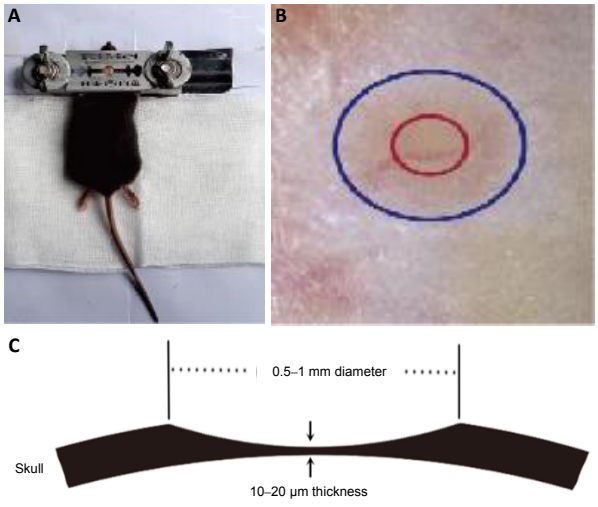

Figure 2 | **Protocol of head grinding and fixation.**
(A) To minimize the movement artifacts, a custom-built plate and skull holder was used as the immobilization device for the head. (B) The targeted imaging area was marked with red circle. (C) The observed area requires the thickness to be 10 to 20 μm and has a diameter of ~200 μm.

Identification of the hindleg representation in motor cortex
The HL representation was identified by micro-stimulation. Stereotaxis was used for the placement and insertion of electrodes (Shanghai Yuyan Scientific Instrument Company, Shanghai, China) into the motor cortex according to the coordinates of Chapin and Lin (1984) to confirm the desired HL motor area. It was located at 1.5 mm behind the anterior fontanelle and 1.0 mm laterally from the sagittal line. The diameter of the viewing window was about 0.5 to 1 mm. The vasculature pattern indicated by microscopy (Shanghai Terer Optoelectronics Company) held steady for months, thus it was used as the landmark to relocate the targeted imaging area at different imaging times.

Image quantification
The imaging parameters of a two-photon microscopy (Shanghai Terer Optoelectronics Company) were: (i) The wavelength of excitation was 920 nm and the laser power was under 40 mW; (ii) The mode of scanning was XYZ and the objective lens was 25×; (iii) The depth of scanning was under 150 μm and the thickness of scanning was 0.75 μm. The axonal boutons and dendritic spines in the bilateral HL motor cortex were imaged, *in vivo* and bilaterally, on the day before (0 days) SPH and 3 days, 2 weeks and 1 month after SPH (**Figure 3A**).

The methods of data analyses have been described previously (Zhang et al., 2015). A total of 130–170 randomly selected axonal boutons were used to observe in every mouse. The boutons were classified as stable, eliminated or newly formed boutons by comparing the same bouton at different imaging sessions (**Figure 3B**–**E**). The calculation formulae of turnover are as follows:

a) The stable rate (e.g., 3 days) = the number of stable boutons that exist in both images of 0 days and 3 days/the number of boutons that exist in image of 0 days.

b) The rate of newly formed, or eliminated, boutons (e.g., 3 days) = the number of newly formed, or eliminated, boutons (identified from images of 0 days and 3 days) / the number of boutons that exist in image of 0 days (the day before SPH).

About 150–200 spines were randomly selected for observation in each mouse. The turnover of a spine is based on its spatial relationship to adjacent landmarks. The numbers of stable spines, new spines and eliminated spines were calculated by comparing the same position at different imaging sessions. In consideration of the limitation of the lowest resolution of the microscope, changes bigger than the range of 0.7 μm suggests that the spine had definitely changed. When compared with the first image, spines of the second image were classified into eliminated spines or formed spines if they were more than 0.7 μm away from their initial positions (**Figure 3F**–**J**). The calculation formulas of turnover are as follows:

a) The rates of eliminated spines, or new, spines (e.g., 3 days) = the number of eliminated, or newly formed, spines (identified from images of 0 days and 3 days) / the number of spines that existed in the image at 0 days (the day before the SPH);

b) The stable rate (e.g., 3 days) = the number of stable spines that existed in both images of 0 days and 3 days/the number of spines that exist in image of 0 days;

c) The survival rate of stable spines (e.g., 3 days to 2 weeks) = the number of stable spines that exist in each of the images at 0 days, 3 days and 2 weeks / the number of stable spines that exist in both images of 0 days and 3 days;

d) The survival rate of formed spines (e.g., 3 days to 2 weeks) = the number of newly formed spines that exist in images of 0 days, 3 days and 2 weeks / the number of formed spines that exist in images of 0 days and 3 days;

e) The re-emerging rate of eliminated spines (e.g., 3 days to 2 weeks) = the number of eliminated spines identified between the first two images (0 days and 3 days) that recurred in the image at the third image (2 weeks) / the total number of eliminated spines identified between the first two images (0 days and 3 days).

Statistical analysis
SPSS 17.0 software (SPSS, Chicago, IL, USA) was used for data analysis. The results were presented as the mean ± standard error of mean (SEM). Student's *t*-tests, Mann-Whitney *U* test and one-way analysis of variance were used to compare the quantitative data. $P < 0.05$ was considered statistically significant.

Results

Postsynaptic dendritic spines of pyramidal neurons in motor cortex after SPH
To evaluate the potential difference of remodeling between the bilateral HL motor cortex in the control condition, we used the control group in which sham operations were performed (laminectomy of the T11–12 spinal vertebral segments without the hemi-section of the spinal cord). We found that the rates of stable spines, eliminated spines and new spines in the bilateral cortex of the control group were not significantly different over 1 month (**Figure 4A**–**C**). These results indicate that the sham operation led to no significant change in the bilateral HL motor cortex. To facilitate calculation and comparison, the integrated results from the control group were the bilateral averages of cortices.

Compared with the control group, stable dendritic spines of ipsi- and contra-lateral cortex in the SPH group were significantly reduced after SPH, especially at 2 weeks after SPH ($P < 0.01$, $n = 6$; **Figure 4D**). This suggests that the SPH led to the reorganization of synaptic connections bilaterally in the HL motor cortex and the peak time of remodeling was 2 weeks after SPH. The elimination of spines in the cortex bilaterally increased significantly after SPH, especially at 2 weeks after SPH ($P < 0.01$ *vs*. control group, $n = 6$; **Figure 4E**). The rates of new spines in the contralateral cortex of SPH group at 1 month were significantly increased when compared with those of the control group and the ipsilateral cortex of SPH group ($P < 0.05$, $n = 6$; **Figure 4F**). It showed that new spines were formed mainly in the contralateral motor cortex after SPH.

To explore how SPH affected the stability of stable spines and new spines and the re-emergent rates of previous eliminated spines in the cortex bilaterally, we examined the survival rates of different kinds of spines. We found that from 3 days to 2 weeks after SPH, the survival rates of stable spines in the cortex were lower bilaterally than those of the control group ($P < 0.05$, $n = 6$; **Figure 5A**). Notably, the re-emergent rates of eliminated spines in both halves of the cortex were lower than those of the control group ($P < 0.05$). From 2 weeks to 1 month, the survival rate of new spines in the contralateral motor cortex of the SPH group was significantly lower than that of the control group ($P < 0.01$, $n = 6$; **Figure 5B**). Comparisons between the results from the contralateral and ipsilateral cortices in the SPH group were not statistically significant ($P > 0.05$, $n = 6$; **Figure 5**).These results indicate that from 3 days to 2 months after SPH, the traditionally stable spines became unstable and the eliminated spines were less likely to re-emerge. Furthermore, the low survival rate of these new spines (which was significantly poorer in the contralateral cortex of SPH group compared with the other groups) shows that new spines are unstable from 2 weeks to 1 month after SPH.

Presynaptic axonal boutons in spines of pyramidal neurons in the HL motor cortex after SPH

To evaluate the potential difference between the cortex of the control group, we evaluated the stable rate, elimination rate and newly formed rate of axonal boutons in the HL motor cortex bilaterally. We found no significant change over 1 month (**Figure 6A**–**C**). To facilitate calculation and comparison, the results of control group cortices were the averaged bilaterally.

Unlike the data of dendritic spine, we found no significant turnover of axonal boutons over the 1 month after SPH (at 3 days: $P > 0.05$ (Mann-Whitney U test), at 2 weeks and 1 month: $P > 0.05$ (one-way analysis of variance); **Figure 6D**–**F**). Combined with the results of spines, it could be concluded that SPH affected postsynaptic dendritic spines rather than presynaptic axonal boutons. Axonal boutons are more stable than dendritic spines after SPH.

Assessment of functional recovery after SPH

To assess the function of the mice, mean BMS for locomotion and BMS subscores for locomotion were used over 1 month. The HL function of the SPH group deteriorated immediately after SPH. HL function showed no obvious recovery during the 1 month time period. The BMS scores of the ipsilateral SPH group are significantly lower than that of other groups over 1 month (12 hours and 1 month: $P < 0.01$ (Student's t-test), 3 days and 2 weeks: $P < 0.01$ (Mann-Whitney U test); **Figure 7A**). The BMS subscores of the SPH group are significantly lower than that of the control groups over 1 month ($P < 0.01$ (Mann-Whitney U test); **Figure 7B**). From the initial SPH to 2 weeks after SPH, the BMS scores and BMS subscores remained close to zero, during which time dendritic spines in bilateral motor cortex decreased. From 2 weeks to 1 month after SPH, the BMS scores and BMS subscores gradually increased, coinciding with the increase in the number of new spines in contralateral motor cortex.

Discussion

For the first time, our data shows that the remodeling of motor cortex after SPH involves postsynaptic spines rather than presynaptic boutons. It indicates that boutons are more stable than spines, which is supported by a study of learning and memory (Majewska et al., 2006; Xiong et al., 2019). It is relevant that new spines often contact boutons that are already in contact with other dendritic spines. Fluctuation in dendritic spine connections with a bouton control the activity of neuronal signal all the way to function (Shepherd and Harris, 1998; Toni et al., 1999, 2007; Knott et al., 2006). A small turnover in such boutons may lead to the turnover of many dendrites spines, which might explain why boutons are appear more stable than spines (Qiao et al., 2016). Rapid, significant spinogenesis was not found during the first 3 days after SPH. Two weeks after SPH, the neural circuits remodeled by eliminating spines in motor cortex bilaterally. One month after SPH, it remodeled principally by forming new spines in the contralateral motor cortex. Our results are partially consistent with an *in vitro* study which found that spine density in the motor cortex decreased initially and partially recovered later on after SCI (Kim et al., 2006). It is important to note that the change of general density observed in previous *in vitro* research was just a kind of endpoint measure. Our *in vivo* study showed that new spines formed at the same time as old spines were eliminated. Furthermore, the survival rate data of previously stable spines and new spines and the rate of re-emergence of previously eliminated spines after SPH had not been demonstrated previously. The data of survival rate in spines showed that the SPH made traditionally stable spines vulnerable, and the re-emergence of eliminated spines became more difficult in the motor cortex bilaterally. Although there was a significant increase in new spines in the contralateral motor cortex, their low survival rate demonstrated that the new spines were still unstable. Our results demonstrate an important anatomical mechanism for the recovery after SCI, which has an important implication for tracking treatment-induced changes and the development of evidence-based rehabilitation therapy (Nardone et al., 2018).

The dynamic remodeling of spines indicates that the SPH changed the pathological structural properties of the motor cortex. The remodeling after SPH occurred bilaterally but not equally over time. From 3 days to 2 weeks after SPH, the loss of spines principally occurred bilaterally in the HL motor cortex. One month after SPH, it remodeled principally in the contralateral motor cortex. Our results are consistent with two earlier studies. One study demonstrated that the recovery of SCI in the early recovery stage involved bilateral motor cortex and more extensive regions of the contra-lesioned cortex and bilateral cortex during the late recovery stage (Nishimura et al., 2007). The other demonstrated that activation of the bilateral motor cortex increased in the early stage and that activation of the contralateral cortex increased in the later stage (Murata et al., 2015).

What caused the differential variation of remodeling in bilateral motor cortex? Different outputs and inputs caused by the disruption of delicate balance of the messaging transmission system between the brain and extremities by SPH may be the reason. The stability of the dendritic spine provides the basis for the brain to store long-term memories (Yu and Zuo, 2011), and the instability of spines leads to their elimination when they no longer receive signals after the loss of motor function. The plasticity of the spine provides the brain with the ability to respond to new experiences (Yu and Zuo, 2011) and early functional recovery depends strongly on increased activity in the motor cortex (Nishimura et al., 2007). Several mechanisms, such as synaptic pruning (Kim et al., 2006), new connections due to dendritic and axonal sprouting (Tan and Waxman, 2012) and neuronal death (Feringa et al., 1984), may contribute to cortical remodeling after SCI. Some studies suspected that the reactivation of dormant synapses after SCI was the underlying mechanism of remodeling in the cortex but was not found in this *in vivo* study. Jurkiewicz et al. (2006) demonstrated morphologic changes and remodeling after SCI was associated with axonal sprouting. Our *in vivo* study found that postsynaptic spines rather than axonal boutons contributed to the cortical remodeling. This difference may be explained by the differences in the lesion model and the severity of behavioral impairment or the method of research (Nishimura et al., 2007).

The limitation of our study is that only a proportion of the neurons are corticospinal neurons in layer V of the motor cortex for YFP-H line transgenic mice and it will be crucial to explore whether synaptic structural plasticity happens in other cell types or layers. Our data provides a structural foundation for understanding remodeling in the motor cortex after SPH. Further investigation into the roles of new spines and stable spines and functional regulatory mechanisms will provide substantial prospects for future SCI studies.

Author contributions: *Study design and manuscript editing: JYC, WC; experimental implementation: KXZ, JJZ. All authors approved the final version of the paper.*

Conflicts of interest: *The authors declare that there is no conflict of interests.*

Financial support: *This work was supported by grants of Foundation and Strengthening Program in Technical Area of China, No. 2019-JCJQ-JJ-149 (to KXZ); and Military Medical Youth Program of Chinese PLA General Hospital, No. QNF19056 (to KXZ). The funding bodies played no role in the study design, in the collection, analysis and interpretation of data, in the writing of the paper, or in the decision to submit the paper for publication.*

Institutional review board statement: *This study was approved by the Ethics Committee of General Hospital of Chinese People's Liberation Army (approval No. 201504168S) on April 16, 2015.*

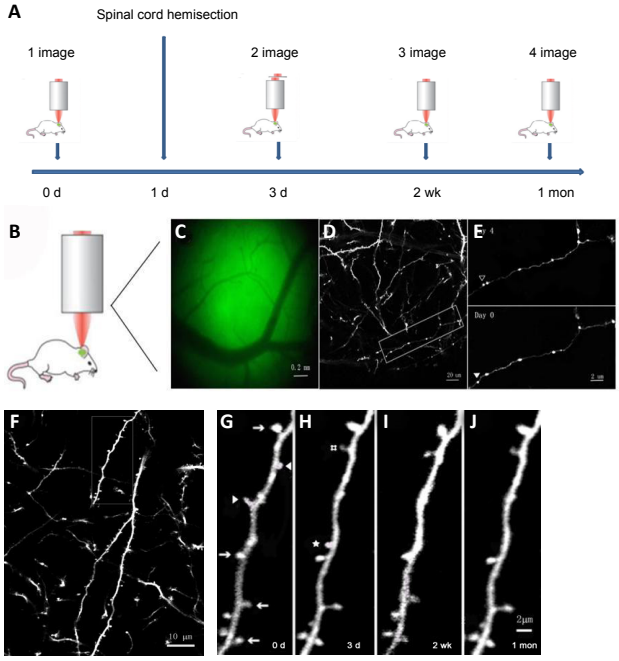

Figure 3 | Identification and calculation methods for the turnover of boutons and spines of pyramidal neurons in motor cortex.
(A) Schematic of the imaging process. (B, C) The vasculature under the thinned skull was used to locate the observation site in all imaging sessions. (D) The imaging of 25× magnification, the axonal boutons and spines were displayed clearly. (E) Repeated imaging of boutons in hindlimb motor cortex at day 0 and day 3 in the magnified area (white box) in D. The open arrowhead indicates the bouton which was eliminated. The filled arrowhead indicates a new bouton which was formed. (F) The imaging of 25× magnification, the spines were displayed clearly. (G–J) Magnified images (white rectangle of F) at 0 days (G), 3 days (H), 2 weeks (I), and 1 month (J). Arrows indicate the spine existed in all imaging sessions. Arrowheads indicate spines that were eliminated. # Indicates the spine which was newly formed in imaging of 3 days and remained at 2 weeks and 1 month. ☆ Indicates the spine, which was newly formed in imaging of 3 days, but disappeared at 2 weeks. Scale bars: 0.2 mm in C, 20 μm in D, 2 μm in E, 10 μm in F, and 2 μm in G–J.

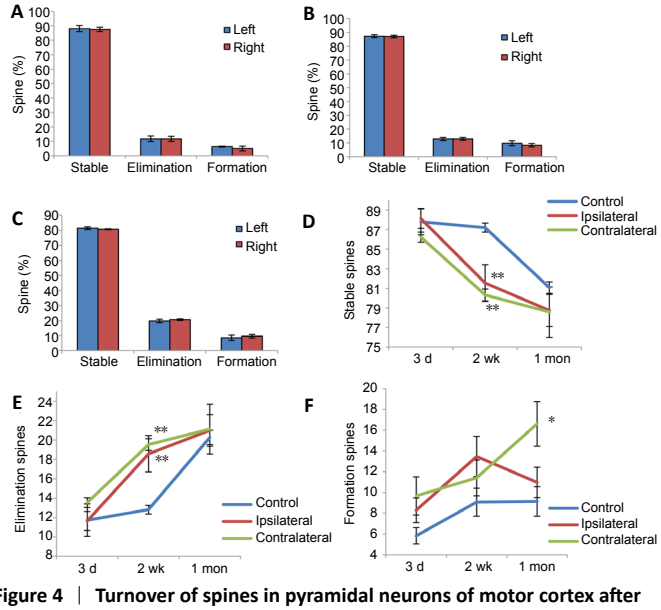

Figure 4 | Turnover of spines in pyramidal neurons of motor cortex after spinal cord hemi-section.
(A–C) The spine turnover of bilateral cortex in the control group after 3 days (A), 2 weeks (B) and 1 month (C). The ipsilateral and contralateral cortex behaved similarly. Hence results from the control group were combined when illustrated in D–F. (D–F) The turnover of stable spines (D), eliminated spines (E), and new spines (F) in both control and spinal cord hemi-section groups over time. All data were presented as the mean ± SEM. *P < 0.05, **P < 0.01 (Student's t-test).

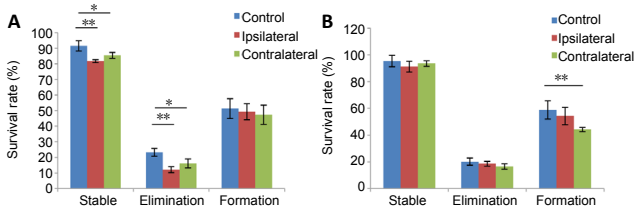

Figure 5 | Turnover of survival rates in spines of pyramidal neurons in the hindimb motor cortex after spinal cord hemi-section.
(A, B) Survival rates of spines calculated from 3 days to 2 weeks (A) and from 2 weeks to 1 month (B). Data are presented as the mean ± SEM (n = 6). *P < 0.05, **P < 0.01 (Student's t-test).

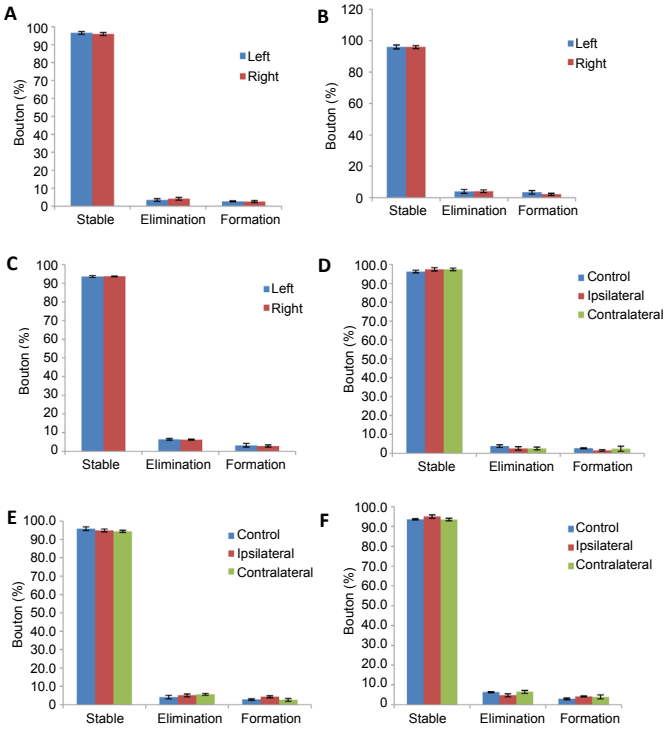

Figure 6 | Turnover of axonal boutons of pyramidal neurons in motor cortex after spinal cord hemi-section.
(A–C) The turnover of the axonal boutons at 3 days (A), 2 weeks (B) and 1 month (C) after laminectomy surgery in the control group. There were no significant difference among these time points (P > 0.05, respectively, n = 6). (D–F) The turnover of boutons at 3 days (D), 2 weeks (E) and 1 month (F) after spinal cord hemi-section in spinal cord hemi-section and control groups. There were no significant difference among these time points (P > 0.05, respectively, n = 6). Data are presented as the mean ± SEM, analyzed by the Mann-Whitney U test (at 3 days) or one-way analysis of variance (at 2 weeks and 1 month).

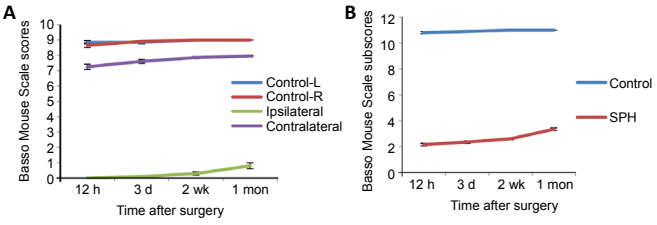

Figure 7 | Basso Mouse Scale scores for locomotion and Basso Mouse Scale subscores for locomotion of SPH rats over a recovery period of 1 month.
(A) Compared with the ipsilateral hindlimb data in the SPH group, pronounced differences in scores occurred in the other three groups at all time points (P < 0.01, n = 6). Compared with the contralateral hindlimb data in the SPH group, pronounced differences in scores occurred in the other three groups at all time points (P < 0.01, n = 6). (B) Compared with the data in control group, pronounced differences in Basso Mouse Scale subscores occurred in the SPH group at all time points (P < 0.01, n = 6). All data were presented as the mean ± SEM, and analyzed by Mann-Whitney U test (3 days and 2 weeks in BMS scores and all timepoints in BMS subscores) or Student's t-test (12 hours and 1 month in Basso Mouse Scale scores). SPH: Spinal cord hemi-section.

Data sharing statement: *Datasets analyzed during the current study are available from the corresponding author on reasonable request.*
Plagiarism check: *Checked twice by iThenticate.*
Peer review: *Externally peer reviewed.*

References

Basso DM, Fisher LC, Anderson AJ, Jakeman LB, McTigue DM, Popovich PG (2006) Basso Mouse Scale for locomotion detects differences in recovery after spinal cord injury in five common mouse strains. J Neurotrauma 23:635-659.

Brown AR, Martinez M (2019) From cortex to cord: motor circuit plasticity after spinal cord injury. Neural Regen Res 14:2054-2062.

Cao JL, Li Q, Wang YJ (2015) Directional and specific characteristics of astrocyte fiber growth and synapse formation. Zhongguo Zuzhi Gongcheng Yanjiu 19:6787-6792.

Chapin JK, Lin CS (1984) Mapping the body representation in the SI cortex of anesthetized and awake rats. J Comp Neurol 229:199-213.

Chen Y, Wang Y, Ertürk A, Kallop D, Jiang Z, Weimer RM, Kaminker J, Sheng M (2014) Activity-induced Nr4a1 regulates spine density and distribution pattern of excitatory synapses in pyramidal neurons. Neuron 83:431-443.

Feringa ER, Gilbertie WJ, Vahlsing HL (1984) Histologic evidence for death of cortical neurons after spinal cord transection. Neurology 34:1002-1006.

Ghosh A, Peduzzi S, Snyder M, Schneider R, Starkey M, Schwab ME (2012) Heterogeneous spine loss in layer 5 cortical neurons after spinal cord injury. Cereb Cortex 22:1309-1317.

Grau JW, Baine RE, Bean PA, Davis JA, Fauss GN, Henwood MK, Hudson KE, Johnston DT, Tarbet MM, Strain MM (2020) Learning to promote recovery after spinal cord injury. Exp Neurol 330:113334.

Grutzendler J, Kasthuri N, Gan WB (2002) Long-term dendritic spine stability in the adult cortex. Nature 420:812-816.

Harms KJ, Dunaevsky A (2007) Dendritic spine plasticity: looking beyond development. Brain Res 1184:65-71.

Hu Y, Guo TC, Zhang XY, Tian J, Lu YS (2019) Paired associative stimulation improves synaptic plasticity and functional outcomes after cerebral ischemia. Neural Regen Res 14:1968-1976.

Isa T (2017) The brain is needed to cure spinal cord injury. Trends Neurosci 40:625-636.

Johnston MV (2009) Plasticity in the developing brain: implications for rehabilitation. Dev Disabil Res Rev 15:94-101.

Jurkiewicz MT, Crawley AP, Verrier MC, Fehlings MG, Mikulis DJ (2006) Somatosensory cortical atrophy after spinal cord injury: a voxel-based morphometry study. Neurology 66:762-764.

Kim BG, Dai HN, McAtee M, Bregman BS (2008) Modulation of dendritic spine remodeling in the motor cortex following spinal cord injury: effects of environmental enrichment and combinatorial treatment with transplants and neurotrophin-3. J Comp Neurol 508:473-486.

Kim BG, Dai HN, McAtee M, Vicini S, Bregman BS (2006) Remodeling of synaptic structures in the motor cortex following spinal cord injury. Exp Neurol 198:401-415.

Knott GW, Holtmaat A, Wilbrecht L, Welker E, Svoboda K (2006) Spine growth precedes synapse formation in the adult neocortex in vivo. Nat Neurosci 9:1117-1124.

Kramer JL, Lammertse DP, Schubert M, Curt A, Steeves JD (2012) Relationship between motor recovery and independence after sensorimotor-complete cervical spinal cord injury. Neurorehabil Neural Repair 26:1064-1071.

Lai CSW, Adler A, Gan WB (2018) Fear extinction reverses dendritic spine formation induced by fear conditioning in the mouse auditory cortex. Proc Natl Acad Sci U S A 115:9306-9311.

Lemtiri-Chlieh F, Zhao L, Kiraly DD, Eipper BA, Mains RE, Levine ES (2011) Kalirin-7 is necessary for normal NMDA receptor-dependent synaptic plasticity. BMC Neurosci 12:126.

Li B, Woo RS, Mei L, Malinow R (2007) The neuregulin-1 receptor erbB4 controls glutamatergic synapse maturation and plasticity. Neuron 54:583-597.

Majewska AK, Newton JR, Sur M (2006) Remodeling of synaptic structure in sensory cortical areas in vivo. J Neurosci 26:3021-3029.

Murata Y, Higo N, Hayashi T, Nishimura Y, Sugiyama Y, Oishi T, Tsukada H, Isa T, Onoe H (2015) Temporal plasticity involved in recovery from manual dexterity deficit after motor cortex lesion in macaque monkeys. J Neurosci 35:84-95.

Nardone R, Höller Y, Sebastianelli L, Versace V, Saltuari L, Brigo F, Lochner P, Trinka E (2018) Cortical morphometric changes after spinal cord injury. Brain Res Bull 137:107-119.

Nishimura Y, Onoe H, Morichika Y, Perfiliev S, Tsukada H, Isa T (2007) Time-dependent central compensatory mechanisms of finger dexterity after spinal cord injury. Science 318:1150-1155.

Pan F, Gan WB (2008) Two-photon imaging of dendritic spine development in the mouse cortex. Dev Neurobiol 68:771-778.

Qiao Q, Ma L, Li W, Tsai JW, Yang G, Gan WB (2016) Long-term stability of axonal boutons in the mouse barrel cortex. Dev Neurobiol 76:252-261.

Segal M (2005) Dendritic spines and long-term plasticity. Nat Rev Neurosci 6:277-284.

Shepherd GM, Harris KM (1998) Three-dimensional structure and composition of CA3-->CA1 axons in rat hippocampal slices: implications for presynaptic connectivity and compartmentalization. J Neurosci 18:8300-8310.

Tada T, Sheng M (2006) Molecular mechanisms of dendritic spine morphogenesis. Curr Opin Neurobiol 16:95-101.

Tan AM, Waxman SG (2012) Spinal cord injury, dendritic spine remodeling, and spinal memory mechanisms. Exp Neurol 235:142-151.

Toni N, Buchs PA, Nikonenko I, Bron CR, Muller D (1999) LTP promotes formation of multiple spine synapses between a single axon terminal and a dendrite. Nature 402:421-425.

Toni N, Teng EM, Bushong EA, Aimone JB, Zhao C, Consiglio A, van Praag H, Martone ME, Ellisman MH, Gage FH (2007) Synapse formation on neurons born in the adult hippocampus. Nat Neurosci 10:727-734.

Xiong Y, Mahmood A, Chopp M (2019) Remodeling dendritic spines for treatment of traumatic brain injury. Neural Regen Res 14:1477-1480.

Xu Z, Adler A, Li H, Pérez-Cuesta LM, Lai B, Li W, Gan WB (2019) Fear conditioning and extinction induce opposing changes in dendritic spine remodeling and somatic activity of layer 5 pyramidal neurons in the mouse motor cortex. Sci Rep 9:4619.

Yu X, Zuo Y (2011) Spine plasticity in the motor cortex. Curr Opin Neurobiol 21:169-174.

Zhang B, Bailey WM, Kopper TJ, Orr MB, Feola DJ, Gensel JC (2015) Azithromycin drives alternative macrophage activation and improves recovery and tissue sparing in contusion spinal cord injury. J Neuroinflammation 12:218.

C-Editor: Zhao M; S-Editors: Yu J, Li CH; L-Editors: Dawes EA, Yu J, Song CP; T-Editor: Jia Y